

1 Trace Measurements of Ethylene Oxide using Cavity-enhanced 2 Absorption Spectrometry near 3066 cm⁻¹

3 Manish Gupta*, Andrew P. Chan, Michael N. Sullivan, and Rupal M. Gupta
4 Nikira Labs Inc., 1074 Wentworth St. Unit B, Mountain View, CA 94043
5 manish.gupta@nikiralabs.com

6 Abstract

7 Ethylene oxide (EtO) is a key carcinogen that is widely used in chemical manufacturing and
8 biotechnology industries. Recent work has suggested that permissible exposure limits for EtO be
9 reduced from 1 – 5 ppm to sub-ppb levels. Such new standards will require new methodologies
10 that are capable of measuring EtO with the requisite precision. In this paper, we demonstrate a new
11 analyzer based on cavity-enhanced absorption spectrometry that utilizes a broad EtO absorption
12 feature near 3066 cm⁻¹. A fit function is developed that includes water, methane, and EtO
13 absorbances and accounts for absorption both inside and outside the cavity. A methane standard is
14 used to determine the cavity gain factor, and the EtO absorbance spectrum is empirically
15 determined. The final system shows excellent linearity from 0 – 909 ppb EtO ($R^2 \sim 0.9999$) with
16 a measurement precision of better than ± 1 ppb (1σ , 60 seconds) that improved to ± 0.5 ppb (1σ , 15
17 minutes). Deliberate ambient EtO releases demonstrate the instrument's utility in rapidly detecting
18 hazardous conditions. Further work will include improving the measurement precision and directly
19 comparing the system to EPA Method TO-15.

20

21 Keywords: Ethylene Oxide, Cavity Ringdown, ICOS, EtO

22 1. Introduction

23 In 2018, 2.92M metric tons of ethylene oxide (EtO) was produced in the United States¹. Most of
24 this EtO was used as an intermediate chemical to produce glycols, ethoxylates, and ethanolamines.
25 Additionally, it was also used in medical sterilization and the food industry. It has long been known
26 that EtO is a carcinogen^{2,3}, and the Occupational Safety and Health Administration (OSHA) has
27 set permissible 8-hour and 15-minute exposure limits of 1 ppm and 5 ppm respectively⁴. After an
28 extensive review of the available data, the US Environmental Protection Agency (EPA) Integrated
29 Risk Information System (IRIA) program concluded⁵ that the “...confidence in the hazard
30 characterization of EtO as ‘carcinogenic to humans’ is high.” Using this data, the EPA has
31 assigned a total cancer unit risk (inhalation unit risk) estimate⁶ for EtO of $3.3 \times 10^{-3} \mu\text{g}/\text{m}^3$ (~12
32 ppt), though recent studies^{7,8} suggests that this unit risk estimate may be too low and a value of ~2
33 ppb may be more appropriate.

34
35 These new standards will require new measurement technologies. Currently, EtO is measured via
36 EPA Methods^{9,10} TO-15 and TO-15A. Briefly, a discrete air sample is captured in a Summa
37 canister¹¹ and shipped to a laboratory for analysis. The canister contents are directed through a
38 solid adsorbent which preconcentrates the volatile organic compounds (e.g. EtO) as well as some
39 common air constituents (e.g. CO₂). Cryogenic cooling is then used to remove most of the CO₂
40 prior to compound separation via a gas chromatography column. Finally, the EtO concentration is
41 measured via selective ion or scanning mass spectrometry.

42
43 Though this method is extensively used, it has several limitations that make it difficult to address
44 emerging EPA need to measure low ppt-levels of EtO. Foremost, EtO is typically characterized by

45 major m/z peaks at 44 and 29, which are confounded by CO₂ and co-eluting species (e.g. trans-2-
46 butene, acetaldehyde, and potentially others) respectively. This limitation can be partially
47 overcome by minimizing leaks, using a longer column, and exploiting other m/z peaks at 15, 41 –
48 43 and 56; however, this reduces the sensitivity of the analysis, making it unable to quantify low
49 levels of EtO. An extensive study¹² of ethylene oxide monitoring using EPA Method TO-15A
50 showed that Summa canister samples filled with dry nitrogen are stable for up to 15 days and can
51 provide EtO detection limits of 0.25 ppb, which is approximately 10 – 20 times higher than the
52 EPA targets noted above. Moreover, EtO production was observed in blank canisters filled with
53 humid air at 50% relative humidity¹³. Though mitigated by an extensive cleaning procedure, this
54 production mechanism produced 0.5 – 1 ppb of EtO in a standard canister in 1 – 2 weeks of storage.
55 In addition to sensitivity, cross-interference, and storage issues, EPA Method TO-15 requires the
56 acquisition and transport of discrete air samples. Thus, the measurement is not real-time or
57 continuous and may not be representative of actual, average EtO concentrations. Finally, as
58 described above, accurate and sensitive EtO analysis requires extensive infrastructure and
59 expertise, making it more complex and expensive.

60

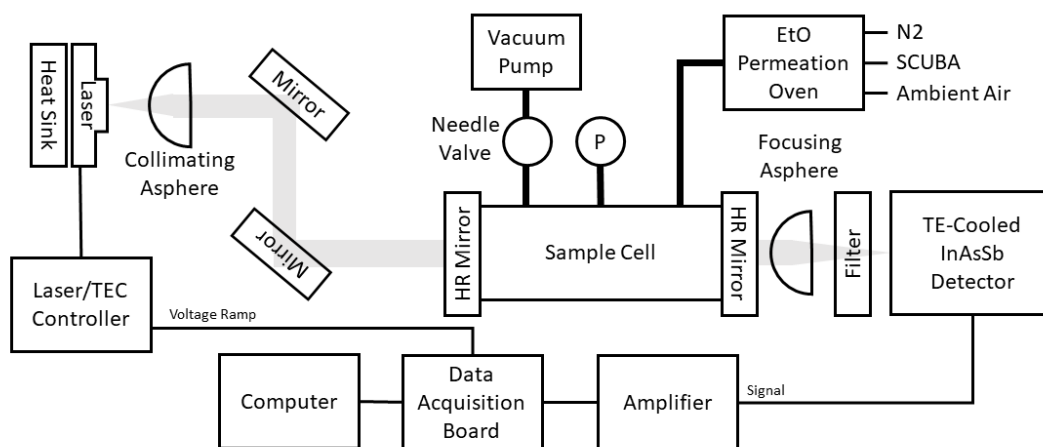
61 There are several alternatives to EPA Method TO-15 that provide real-time EtO measurements,
62 including EPA Methods TO-18, 320, and 25A that use online gas chromatography, Fourier
63 Transform Infrared (FTIR), and flame ionization detection respectively. However, all these
64 methods suffer from limited sensitivity and cross-interference¹⁴. Recently, near-infrared cavity
65 ringdown spectroscopy has been used to quantify EtO at the ppb-level¹⁵, and this method may
66 prove to be useful for source monitoring.

67

68 In this paper, we present an ethylene oxide analyzer based on cavity-enhanced absorption
 69 spectrometry near 3066 cm^{-1} that is capable of making real-time measurements with sub-ppb
 70 precision. Previously, high-resolution FTIR spectra of ethylene oxide^{16,17} show strong absorption
 71 features near 3060 cm^{-1} and 1270 cm^{-1} ; however, tunable diode laser absorption spectrometry has
 72 only been used¹⁸ near 5907 cm^{-1} . This latter work showed a precision of 17 ppm (1σ) using a 63.5
 73 cm cell and extrapolated to a measurement precision of 30 ppb assuming a much longer pathlength
 74 (100 meters) and 10x reduction in noise using wavelength modulation spectroscopy. In this work
 75 we achieve a measurement precision of better than $\pm 1\text{ ppb}$ (1σ , 60 seconds) by using a substantially
 76 stronger absorption feature and a high-finesse cavity to provide a very long effective pathlength.
 77

78 2. Methods

79 2.1 Experimental Setup



80

81 **Figure 1: Schematic overview of experimental setup.**

82

83 The experimental setup is shown schematically in Figure 1. A 25 mW distributed feedback DFB
84 diode laser with incorporated TEC operating near 3066 cm^{-1} (3262 nm) with a linewidth of ~ 3
85 MHz (0.0001 cm^{-1}) at $6\text{ }^{\circ}\text{C}$ (Nanoplus GmbH) is mounted onto a heatsink and collimated using an
86 AR-coated asphere (NA = 0.56) mounted on an x/y/z stage. The collimated beam is directed into
87 a high-finesse optical cavity comprised of two highly-reflective, 1-inch diameter mirrors ($R >$
88 99.8% at 3066 cm^{-1} , LayerTec GmbH). In order to minimize coherent interferences within the
89 cavity, the cavity is intentionally misaligned, and the laser beam is slightly defocused akin to
90 Integrated Cavity Output Spectroscopy (ICOS)¹⁹ and off-axis ICOS²⁰. The mid-infrared DFB
91 diode laser was repeatedly tuned over 4 cm^{-1} by varying its injection current from 0 – 150 mA at
92 a rate of 8 kHz. 8000 transmission spectra were averaged prior to analysis, yielding an analyzer
93 data reporting rate of 1 Hz.

94

95 Light transmitted through the cavity is focused by an AR-coated, $f/1$ silicon asphere, passed
96 through an optical filter, and directed onto a thermo-electrically cooled InAsSb detector
97 (Thorlabs). The detector is AC-coupled and provides a gain of 10000 V/A, a responsivity of ~ 1.2
98 A/W at 3263 nm, and a bandwidth of 100 kHz. Note that, due to the low bandwidth of the system,
99 the effective optical pathlength of the cavity cannot be determined by cavity ringdown
100 measurements²¹. Instead, fits to a known absorption are used to determine the cavity gain factor as
101 described below.

102

103 In an ideal incoherent cavity enhanced absorption spectrometry system, approximately $I_0 \cdot T/2$
104 milliwatts of light transmit through the cavity, where $I_0 = 25\text{ mW}$ is the incident laser power and
105 $T \sim 0.1\%$ is the mirror transmission ($T \sim 1 - R$). Thus, in an ideal situation, $\sim 12\text{ }\mu\text{W}$ of laser light

106 would be focused onto the detector, resulting in a peak signal of ~ 140 mV. However, due to large
107 losses in the mirror coatings (e.g. absorption and scatter coatings), the measured detector signal is
108 only a few mV. To avoid limiting the system performance by bit-noise in the data acquisition
109 system, the detector signal is passed through a $10\text{ k}\Omega$ terminator and into an inverting amplifier
110 with a gain of 200. The amplifier output is digitized by a custom data acquisition board at 4 MS/s
111 and collected by a computer. The data acquisition board also provides a voltage ramp with a 90%
112 duty cycle that is connected to a laser driver (Thorlabs) that controls the laser current and
113 temperature.

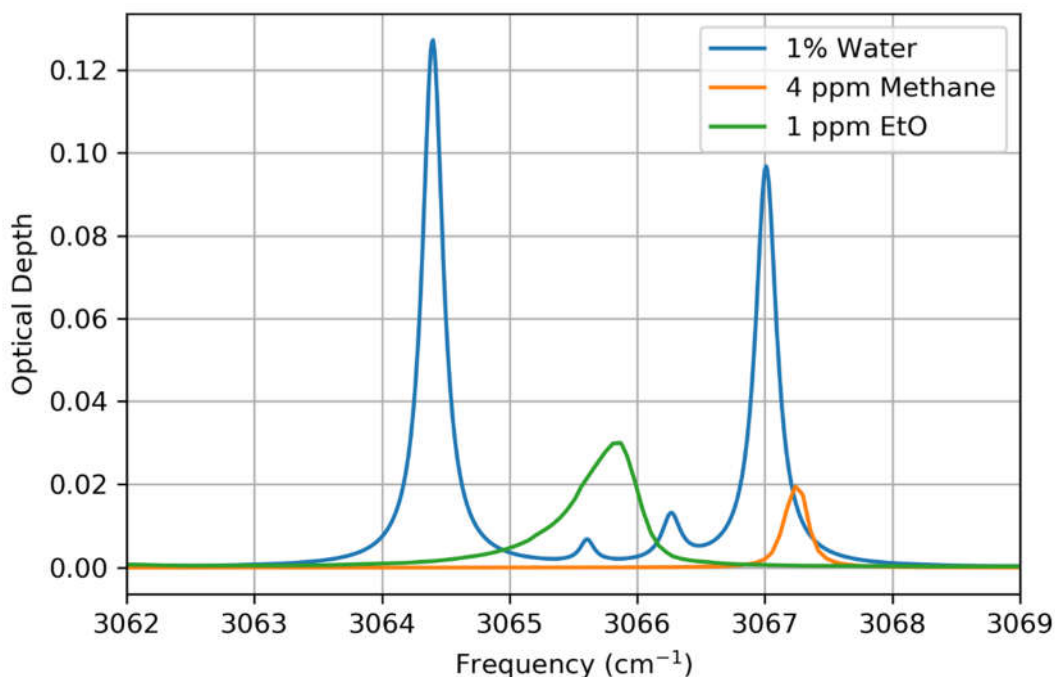
114
115 The gas samples are generated by a programmable permeation oven (VICI Metronics) containing
116 an ethylene oxide permeation tube that provides a permeation rate of 1799 ng/min at $45\text{ }^\circ\text{C}$.
117 Different gases can be flowed through the permeation oven, including nitrogen, SCUBA air,
118 ambient air (pushed by a small diaphragm pump), and $80\text{ ppm CH}_4/\text{N}_2$. The pressure in the cavity
119 is measured by a Baratron pressure gauge (MKS). In order to control the pressure in the cavity and
120 maintain it at $\sim 500\text{ Torr}$, the upstream permeation oven flow rate is set, and gas is pulled through
121 the cavity using a 3-head diaphragm vacuum pump (KNF) whose flow rate is manually controlled
122 by a needle valve.

123

124 2.2 Data Analysis

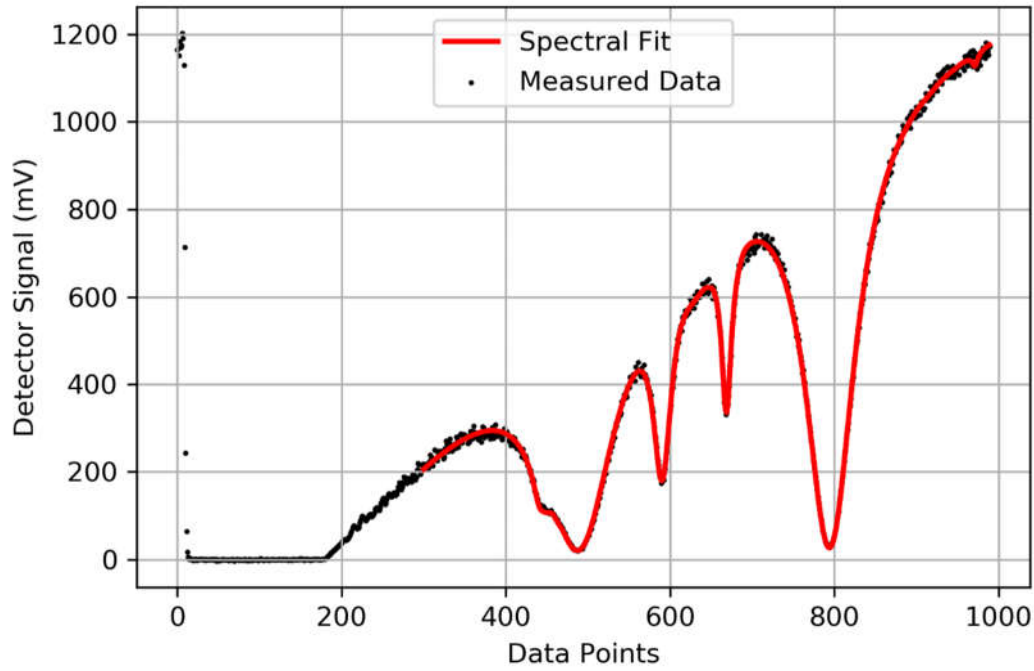
125 Simulated spectra of probe region are shown in Figure 2 for a gas sample containing 1% water
126 vapor, 4 ppm methane, and 1 ppm ethylene oxide. The former was simulated using HITRAN
127 parameters²², whereas the latter two species used data tabulated by Pacific Northwest National
128 Laboratory (PNNL)²³. Note that the entire PNNL and HITRAN databases were surveyed, and no

129 other compounds were found to have absorptions exceeding 0.0002 for 1 ppm compound in a 1-
130 meter pathlength (1/100th the optical depth of ethylene oxide). Thus, we anticipate that the data
131 analysis routine only needs to include water vapor, methane, and ethylene oxide.



132
133 **Figure 2:** Simulated absorption spectra of water vapor (blue), methane (orange), and ethylene oxide
134 (green) in the spectral probe region. Note that no other compounds in the PNNL database
135 were found to absorb in this region.

136
137 A sample measured cavity-enhanced transmission spectrum of ambient air containing ~1.5 %
138 water vapor and ~2 ppm methane is shown in Figure 3. Each data point represents 0.25 μ s,
139 commiserate with the sampling rate. Note that, as expected, the cavity-enhanced transmission
140 spectrum is dominated by water vapor optical absorption.



141
 142 **Figure 3:** Raw measured detector signal (black) with 500 Torr of ambient air in the cavity corrected for
 143 an offset value and fit to the function (red) described in the text. The sampling rate is 4 MHz
 144 (0.25 μ s/datapoint) and 8000 spectra were averaged over 1 second.

145
 146 After subtracting the detector offset, the transmitted intensity, I , is fit to:

147
 148
$$I(x, P_{H_2O}, P_{CH_4}, P_{EtO}) = \frac{I_0(x) * e^{-OD_{outside}}}{(1 + G * OD_{inside})} \quad (1)$$

149
 150 where x is the datapoint (equivalent to the time axis), P is the partial pressure of the indicates
 151 species, $I_0(x)$ is the transmitted intensity in the absence of all absorption (approximated by a 3rd
 152 order polynomial), G is the cavity gain factor, $OD_{outside}$ is the optical depth due to ambient air
 153 absorption of water and methane outside the cavity, and OD_{inside} is the optical depth due to sample
 154 absorption inside the cavity. Equation 1 is a combination of the Beer-Lambert-Bouguer Law and

155 the absorption equation for cavity-enhanced absorption spectrometry²⁰. For water vapor and
156 methane, the optical depth as a function of frequency, f , is expressed using the standard HITRAN²²
157 formulation. For example, for methane, OD(f) is given as:

158

$$159 \quad OD_{CH_4}(f) = P_{CH_4} * N * L * \sum_i S_i * V(f, LW, DW) \quad (2)$$

160

161 where N is a function of temperature, T , and is $2.479e19 * 296/T$, L is the relevant pathlength, S_i is
162 the linestrength of the i^{th} tabulated line, LW is the Lorentz width of the feature, and DW is the
163 Doppler width of the feature (function of total pressure and temperature). A similar expression is
164 used for water vapor. All tabulated line parameters (line frequencies, line strengths, broadening
165 coefficients...) are taken from the HITRAN database²². OD(f) for ethylene oxide is determined by
166 measuring the basis set as described below. The total optical depth is then expressed as the sum of
167 all components.

168

169 Since optical depth is expressed as a function of frequency and the measured intensity is a function
170 of datapoint, the etalon function is approximated as:

171

$$172 \quad f(x) = e_0 + e_1x + e_2x^2 \quad (3)$$

173

174 where e_n are coefficients determined from the fit. Note that, though the actual laser tuning curve is
175 more complex, it can be well approximated by a 2nd-order polynomial over a small tuning range.
176 A more accurate measure of $f(x)$ can be obtained by measuring the laser transmission through a

177 germanium etalon of known length. This method may be employed in the future to further
178 characterize the laser tuning curve.

179
180 Using this fit function, the gas temperature, gas pressure, and pathlength outside the cavity are
181 fixed, whereas the species' partial pressures, baseline coefficients, and etalon coefficients are
182 floated. The cavity gain factor is measured as described below and then fixed for all subsequent
183 analyses.

184
185 In order to limit computational overhead, a subset of the HITRAN database is used to obtain the
186 tabulated parameters. This subset spans from 3061 – 3071 cm^{-1} and only includes water and
187 methane lines with linestrengths greater than 10^{-24} $\text{cm}/\text{molecule}$ and 10^{-22} $\text{cm}/\text{molecule}$
188 respectively.

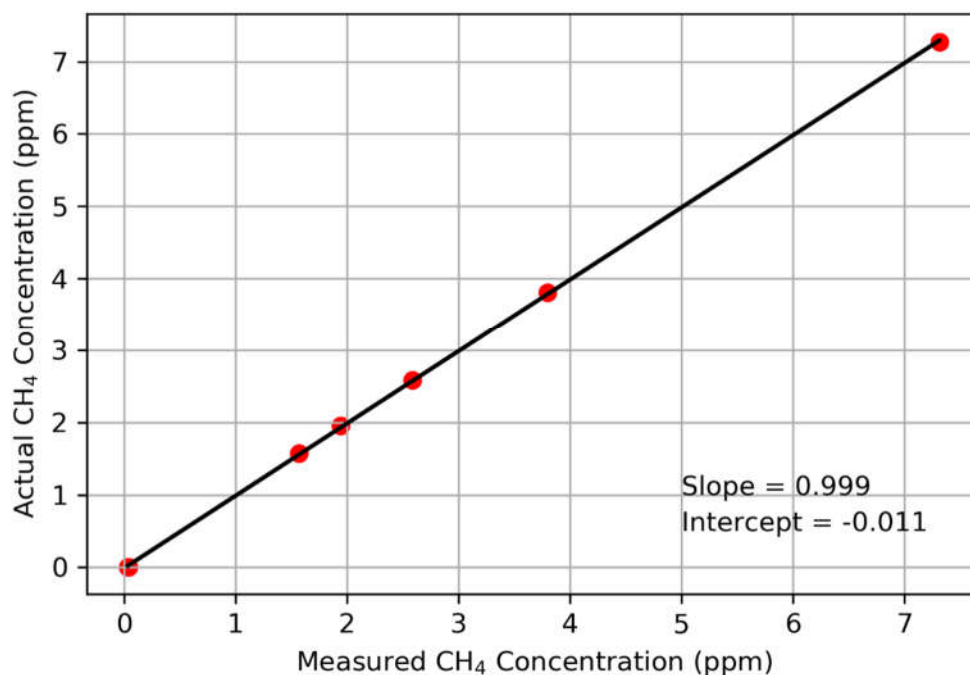
189 190 2.3 Determination of the Cavity Gain Factor

191 The cavity gain factor, G , is typically determined from the mirror reflectivity, R :

192
193
$$G = \frac{R}{1-R} \tag{4}$$

194
195 This reflectivity is usually measured via cavity ringdown spectroscopy²¹ on the empty (or nitrogen-
196 filled) cell. However, due to the limited bandwidth of the detector (100 kHz), the cavity gain factor
197 was determined by measuring dilutions of an 80 ppm $\text{CH}_4/\text{nitrogen}$ standard from 0 – 7.3 ppm.
198 The measured methane concentration (ppm) was then compared to the actual methane
199 concentration and the gain factor was adjusted to yield a slope of ~ 1 . Using this method, we

200 obtained highly linear results with a slope of 0.999 and an intercept of -0.011 by using a gain factor
201 of 740 (Figure 4). This suggests mirror reflectivity $R \sim 99.86\%$, consistent with the manufacturer's
202 indication that $R > 99.7\%$.



203
204 **Figure 4:** By adjusting cavity gain factor to 740, the actual versus measured methane concentration
205 yielded a slope of ~ 1 and an intercept of ~ 0 .

207 2.4 Measuring and Incorporating the Ethylene Oxide (EtO) Basis Set

208 Unlike water and methane, ethylene oxide absorption features are not in the HITRAN database.
209 They have been measured and disseminated by Pacific Northwest National Laboratory (PNNL)²³;
210 however, the FTIR resolution of 0.125 cm^{-1} is insufficient for the high-resolution laser
211 spectrometry presented here. Therefore, measurements of 500 Torr dry nitrogen and 500 Torr of
212 475 ppb EtO/N₂ were used to construct the EtO absorption basis set. The measured dry nitrogen

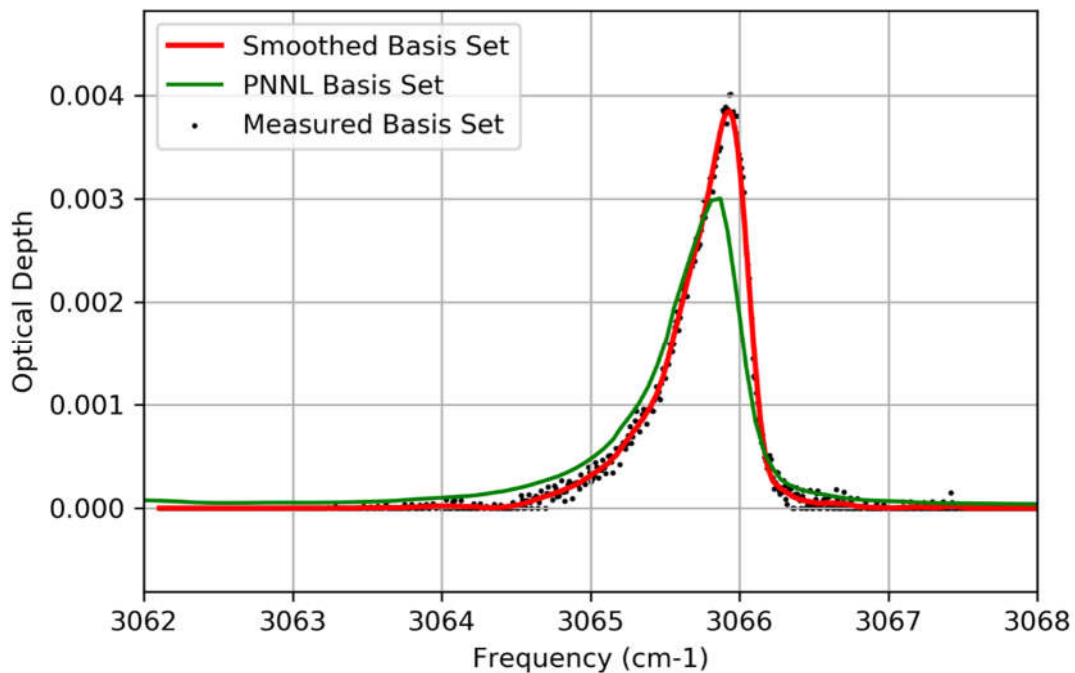
213 transmission spectrum was fit to equation 1 to determine $I_0(x)$. The cavity-enhanced EtO
214 absorbance, A_E , was then determined as:

215

$$216 \quad GA_E = I_0 \left(\frac{1}{I_E} - \frac{1}{I_{N_2}} \right) \quad (5)$$

217

218 where I_E and I_{N_2} are the measured transmission spectra with and without EtO respectively. Finally,
219 a spectrum of ambient air with no EtO was measured and fit to determine the etalon function, $f(x)$.
220 Combining these measurements and smoothing the resulting absorbance spectrum with a 3rd-order
221 Savitzky-Golay filter (boxsize = 41 points) to minimize noise yielded the EtO basis set shown in
222 Figure 5. Note that the data, which has been scaled to represent the absorption of 475 ppb EtO in
223 a 1-meter pathlength, is in good agreement with the PNNL results, but slightly shifted in frequency.



224

225 **Figure 5: Measured (black dots) and smoothed (red) basis set for 475 ppb EtO in a 1-meter pathlength.**

226

The published PNNL FTIR spectrum is included in green.

227

228 This EtO basis set, $B_{EtO}(f)$, was incorporated into the fit by adding an EtO term to the optical depth:

229

$$230 \quad OD_{EtO}(f) = C_{EtO} * B_{EtO}(f) \quad (2)$$

231

232 where C_{EtO} is a coefficient that is proportional to the EtO concentration, and the basis set was

233 linearly interpolated at for all values of f . The relationship between C_{EtO} and the actual

234 concentration of EtO was determined empirically as presented below.

235

236 3. Results and Discussion

237 3.1 Linearity and Relationship between C_{EtO} and EtO Concentration

238 In order to determine the relationship between C_{EtO} and the actual EtO concentration as well as

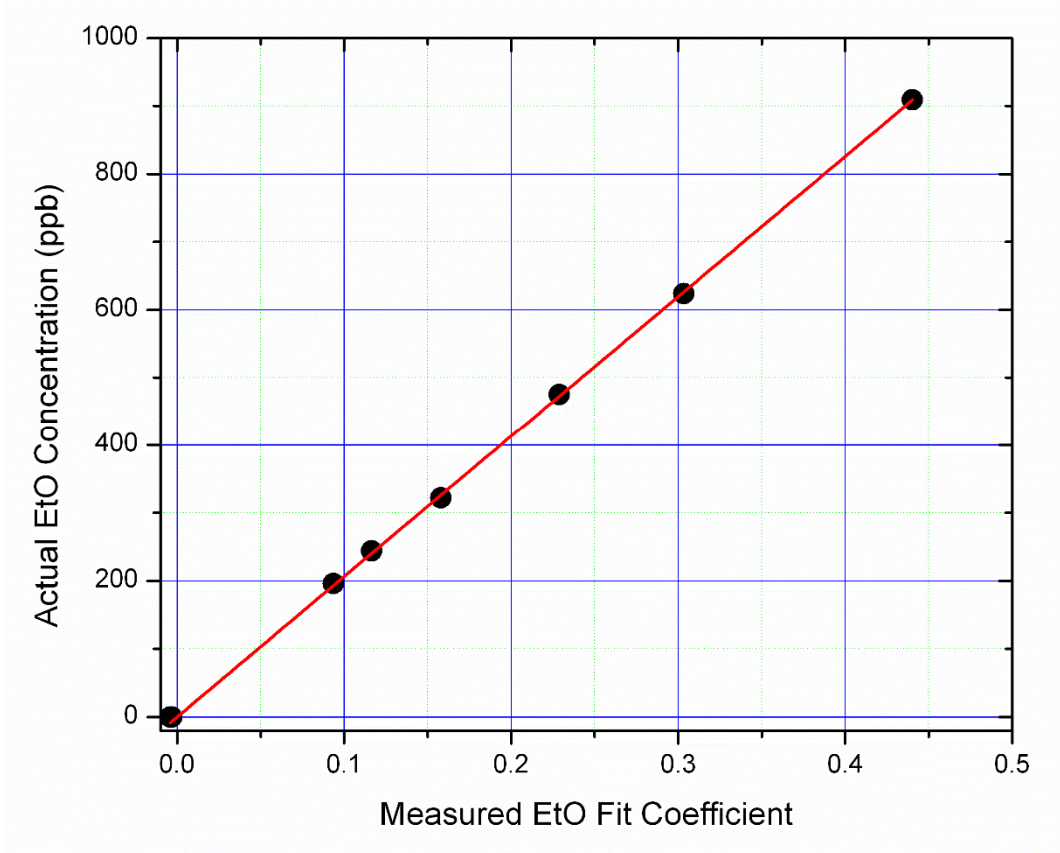
239 gauge the linearity of the analyzer, the permeation oven dilution was adjusted to produce

240 concentrations of EtO ranging from 0 – 909 ppb. The resulting data (Figure 6) was fit to line with

241 zero intercept and yielded a slope of 2064.3 with a $R^2 \sim 0.9999$, suggesting that the analyzer

242 provides a very linear response over this dynamic range. Note that the accuracy of the

243 proportionality coefficient, C_{EtO} , is limited by the accuracy of the permeation tube to $\pm 15\%$.



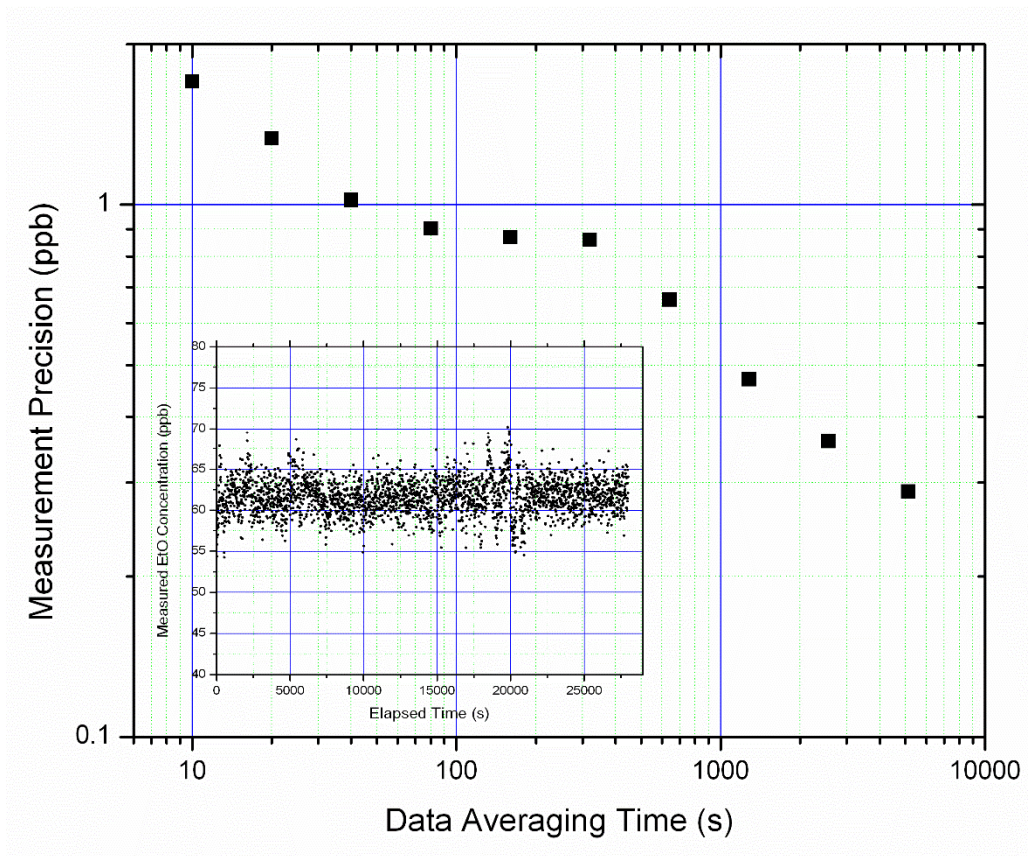
244

245 **Figure 6: Measured EtO coefficient versus actual EtO concentration from 0 – 909 ppb. Note that the**
 246 **analyzer provides a highly linear response ($R^2 \sim 0.9999$) and the slope yields a conversion**
 247 **factor of 2064 between the measured EtO coefficient and EtO concentration.**

248

249 3.2 Measurement Precision

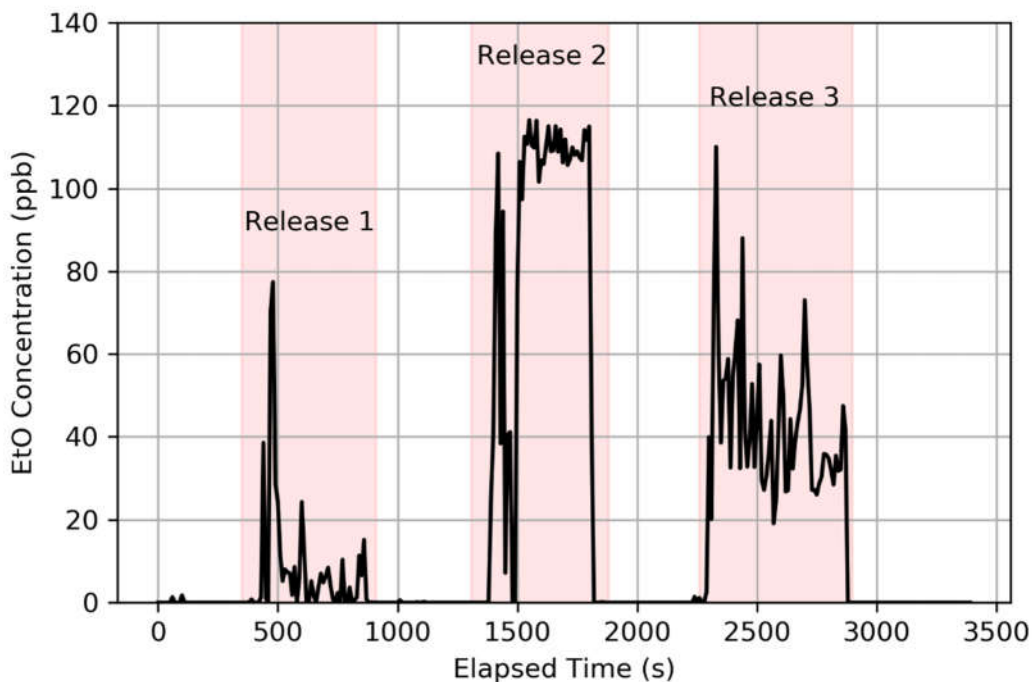
250 The analyzer's measurement precision was determined by continuously measuring a sample of
 251 60.5 ppb EtO/air for ~8 hours. The data and resulting Allan variance are shown in Figure 7. Note
 252 that the system provides a short-term precision of ± 1.7 ppb (1σ , 10 s) that improves to better than
 253 ± 0.5 ppb (1σ) with 15 minutes of averaging. As noted above, this is comparable to EPA Method
 254 TO-15, but provides real-time data with no user intervention.



255
 256 **Figure 7: Allan deviation plot showing the measurement precision as a function of data averaging time.**
 257 **The raw data is shown in the inset.**

258
 259 **3.3 Ambient Air Monitoring**

260 Subsequent to the validation studies above, the analyzer was used to monitor ambient air in the
 261 laboratory during three deliberate ethylene oxide releases from the permeation oven. The cell inlet
 262 was disconnected from the permeation oven and sampled ambient air through a 0.1-micron Teflon
 263 membrane filter. The measured ethylene oxide values as a function of time are shown in Figure 8,
 264 and clearly demonstrate the ability of the system to detect ethylene oxide leaks and hazards at low
 265 levels.



266

267 **Figure 8:** Measured EtO concentrations in ambient air during three deliberate EtO releases

268

269 4. Conclusion and Future Work

270 In this contribution, we have presented the test results of a mid-infrared, cavity-enhanced analyzer
 271 capable of providing real-time, rapid (1 Hz), ppb-level measurements of ethylene oxide. The
 272 technique will enable the accurate quantification of EtO source emissions, as well as enable fast
 273 alarm level measurements in facilities that generate or use large quantities of EtO.

274

275 In order to address next-generation EtO monitoring needs, the instrument precision needs to be
 276 improved by a factor of $\sim 10 - 30$. The methodology presented here can be improved in several
 277 ways to approach this goal. Foremost, the one-inch diameter mirrors can be replaced by two-inch
 278 diameter mirrors. Previous work²⁰ has shown that this decreases the noise of cavity-enhanced
 279 absorption spectrometry by a factor of ~ 10 by providing better incoherent coupling. Likewise,

280 since the system is limited by detector signal and thus requires an external amplifier, a higher
281 power laser, reinjection²⁴, and mirror coatings with less absorption/scatter should also improve the
282 SNR of the analyzer. Finally, a DC-coupled detector may help mitigate long-term changes in
283 baseline curvature. Note that, since water is a strong optical absorber in the spectral
284 region, using higher reflectivity mirrors is not expected to improve the analyzer performance.

285

286 In addition to improving the instrument precision, the system accuracy may be substantially
287 increased by using gravimetric standards or intercomparisons to EPA Method TO-15, instead of
288 permeation tubes. In order to account for changes in temperature and pressure, the EtO basis set
289 can be further developed under different environmental conditions and appropriately interpolated.
290 Finally, the analyzer should be deployed outside, under real-world conditions, and directly
291 compared to EPA Method TO-15.

292

293 5. Acknowledgments

294 We gratefully acknowledge that this work was supported by the EPA SBIR Program under contract
295 number 68HERC21C0016. We also acknowledge Ned Shappley in providing insight into the needs
296 and limitations of current ethylene oxide monitoring as well as helpful comments in preparing this
297 manuscript.

298

299

-
- ¹ American Chemistry Council Economics and Statistics Department (June 2019), “The Economic Benefits of Ethylene Oxide and the Potential Cost of Deselection,” published online at <https://www.americanchemistry.com/EO/Ethylene-Oxide-and-the-Potential-Cost-of-Deselection.pdf>
- ² Hogstedt, C., Aringer, L. and Gustavsson, A., 1986. Epidemiologic support for ethylene oxide as a cancer-causing agent. *Jama*, 255(12), pp.1575-1578.
- ³ Shore, R.E., Gardner, M.J. and Pannett, B., 1993. Ethylene oxide: an assessment of the epidemiological evidence on carcinogenicity. *Occupational and Environmental Medicine*, 50(11), pp.971-997.
- ⁴ OSHA Standard Number 1910.1047 - Ethylene oxide, found at <https://www.osha.gov/laws-regs/regulations/standardnumber/1910/1910.1047>
- ⁵ “Evaluation of the Inhalation Carcinogenicity of Ethylene Oxide,” *Office of Research and Development US Environmental Protection Agency*, Report # EPA/635/R-16/350Fa (December 2016).
- ⁶ “Evaluation of the Inhalation Carcinogenicity of Ethylene Oxide – Executive Summary,” *Office of Research and Development US Environmental Protection Agency*, Report #EPA/635/R-16/350Fc (December 2016).
- ⁷ Vincent, M.J., Kozal, J.S., Thompson, W.J., Maier, A., Dotson, G.S., Best, E.A. and Mundt, K.A., 2019. Ethylene Oxide: Cancer Evidence Integration and Dose–Response Implications. *Dose-Response*, 17(4), p.1559325819888317.
- ⁸ TEXAS COMMISSION ON ENVIRONMENTAL QUALITY, “Ethylene Oxide Carcinogenic Dose-Response Assessment,” CAS Registry Number: 75-21-8 (May, 2020).
- ⁹ “Compendium of Methods for the Determination of Toxic Organic Compounds in Ambient Air – Second Edition,” *Office of Research and Development US Environmental Protection Agency*, Report # EPA/625/R-96/010b (January 1999).
- ¹⁰ “Ethylene Oxide Measurements by TO-15 Method,” Ambient Air Monitoring Group, EPA/OAQPS/AQAD. Found at: <https://www3.epa.gov/ttnamtl1/files/ambient/airtox/EtO-Method-for-NATTS-labs-2019.pdf>
- ¹¹ Note that Summa canister is used as the general term for air capturing canisters and includes other, similar products (e.g. Silonite Ceramic coated canisters).
- ¹² Eklund, B.M., Williams, C.H., Bontempo, L.W., Isbell, M. and Loos, K.R., 2004. Development and validation of a canister method for measuring ethylene oxide in ambient air. *Environmental science & technology*, 38(15), pp.4200-4205.
- ¹³ Hoisington, J. and Herrington, J.S., 2021. Rapid Determination of Ethylene Oxide and 75 VOCs in Ambient Air with Canister Sampling and Associated Growth Issues. *Separations*, 8(3), p.35.
- ¹⁴ Shappley, N. and Yelverton, T., Ethylene Oxide Measurement Research Update presented at the State/USEPA Region 5 Air Toxics Risk Assessment Meeting (November 12th, 2019).
- ¹⁵ Lucic, G., Rella, C., Bent, J. and Schmid, V., 2021, December. Ethylene Oxide and VOC Measurements Using a Cavity Ring-Down Spectrometer (CRDS). In *AGU Fall Meeting 2021*. AGU.
- ¹⁶ Sharpe, S.W., Johnson, T.J., Sams, R.L., Chu, P.M., Rhoderick, G.C. and Johnson, P.A., 2004. Gas-phase databases for quantitative infrared spectroscopy. *Applied spectroscopy*, 58(12), pp.1452-1461.
- ¹⁷ Johnson, T.J., Sams, R.L. and Sharpe, S.W., 2004, March. The PNNL quantitative infrared database for gas-phase sensing: a spectral library for environmental, hazmat, and public safety standoff detection. In *Chemical and Biological Point Sensors for Homeland Defense* (Vol. 5269, pp. 159-167). International Society for Optics and Photonics.
- ¹⁸ Lytkine, A., Jäger, W. and Tulip, J., 2010. Tunable diode laser spectroscopy of ethylene oxide near 1693 nm. *Applied Physics B*, 98(4), pp.871-876.
- ¹⁹ O’Keefe, A., 1998. Integrated cavity output analysis of ultra-weak absorption. *Chemical Physics Letters*, 293(5-6), pp.331-336.
- ²⁰ Baer, D.S., Paul, J.B., Gupta, M. and O’Keefe, A., 2002. Sensitive absorption measurements in the near-infrared region using off-axis integrated-cavity-output spectroscopy. *Applied Physics B*, 75(2), pp.261-265.
- ²¹ O’Keefe, A. and Deacon, D.A., 1988. Cavity ring-down optical spectrometer for absorption measurements using pulsed laser sources. *Review of scientific instruments*, 59(12), pp.2544-2551.
- ²² Rothman, L.S., Gordon, I.E., Barbe, A., Benner, D.C., Bernath, P.F., Birk, M., Boudon, V., Brown, L.R., Campargue, A., Champion, J.P. and Chance, K., 2009. The HITRAN 2008 molecular spectroscopic database. *Journal of Quantitative Spectroscopy and Radiative Transfer*, 110(9-10), pp.533-572.
- ²³ Sharpe, S.W., Johnson, T.J., Sams, R.L., Chu, P.M., Rhoderick, G.C. and Johnson, P.A., 2004. Gas-phase databases for quantitative infrared spectroscopy. *Applied spectroscopy*, 58(12), pp.1452-1461.

²⁴ Leen, J.B. and O'Keefe, A., 2014. Optical re-injection in cavity-enhanced absorption spectroscopy. *Review of Scientific Instruments*, 85(9), p.093101.